Review: Requirements for a Ground Rotation Sensor to Improve Advanced LIGO

by B. Lantz, R. Schofield, B. O'Reilly, D. E. Clark, and D. DeBra

Abstract   The goal of the Laser Interferometer Gravitational-Wave Observatory (LIGO) project is to measure gravitational waves from astrophysical sources. The project has recently begun the construction of Advanced LIGO, a major upgrade to the existing detectors. The performance of the new detectors requires the optical component to be mounted on high performance seismic isolation and alignment systems. The performance and reliability of these isolation systems could be improved with accurate measurements of the tip–tilt rotations of the ground at the level of 3×10^{-10} rad$/\sqrt{\text{Hz}}$ at 10 mHz to 6×10^{-9} rad$/\sqrt{\text{Hz}}$ at 200 mHz. We briefly describe the LIGO project and explain the desire for rotation sensing of the ground. We then derive the performance requirements for a rotation sensor and show that it would improve the Advanced LIGO detector.

## An Introduction to Gravitational Waves and Their Detection

In 1916 Albert Einstein used his new theory of general relativity to describe how the acceleration of massive objects would generate distortions in space-time, which propagate at the speed of light. These gravitational waves provide an explanation of how information about an object's location can be transmitted at a finite speed and provide an answer to the question of why gravity does not generate instantaneous action at a distance. The effect of a gravitational wave is quite difficult to measure directly, and to date there has not been a direct detection of a gravitational wave. The effects of gravitational waves are so small that the most likely source of measurable waves are astrophysical events. Examples of these events include the final inspiral and merger of two neutron stars or two black holes, a stellar core-collapse, which generates a supernova, the periodic signal generated by bumps on the surface of a spinning neutron star, and more exotic sources such as waves left from the first instants after the big bang.

There have been indirect measurements of gravitational waves generated by inspiraling neutron stars. If one (or both) of these neutron stars is a pulsar (therefore emitting regular bursts of radio signals), the orbital evolution of the pair can be tracked over time. Astronomers are now following six of these systems. Perhaps the most famous is the first one to be discovered, which is named PSR 1913 + 16. That work resulted in a Nobel prize for its discoverers, Hulse and Taylor. The orbital decay of the system has been tracked since 1973, and the predicted orbital decay from energy lost to gravitational radiation matches observations to within 1% (Taylor, 1989).

The potential to use gravitational waves to do astronomy has drawn considerable interest to the field. Several projects are now underway to detect gravitational waves. These include several long-baseline laser interferometers such as the Laser Interferometer Gravitational-Wave Observatory (LIGO) project, which is the focus of this article (Barish and Weiss, 1999; Sigg and LIGO Scientific Collaboration, 2008), the German–United Kingdom observatory GEO600 (Grote, 2008), the French–Italian observatory Virgo (Acernese *et al.*, 2008), and the Japanese observatory TAMA (Tatsumi *et al.*, 2007). Several others are in development, such as the Australian Consortium for Interferometric Gravitational Astronomy known as ACIGA (Barriga *et al.*, 2005), the Large-Scale Cryogenic Gravitational-Wave Telescope, or LCGT (Kuroda and The LCGT Collaboration, 2006), and the space-based Laser Interferometer Space Antenna (LISA) mission (Shaddock, 2008). There are also several active bar detectors, but they are beyond the scope of this article. A coordinated network of detectors is a great benefit to the community because it helps distinguish local noise from astrophysically generated signal and, by using time-of-arrival information at widely separated detectors, one can localize the source location on the sky.

Principle of Operation

The long-baseline interferometric gravitational-wave detectors such as LIGO look for gravitational waves by monitoring the distance between separated masses and measuring small variations in the separation, which may be caused by the passage of a wave. Gravitational waves are transverse

T=0	T=P/4	T=P/2	T=3P/4	T=P
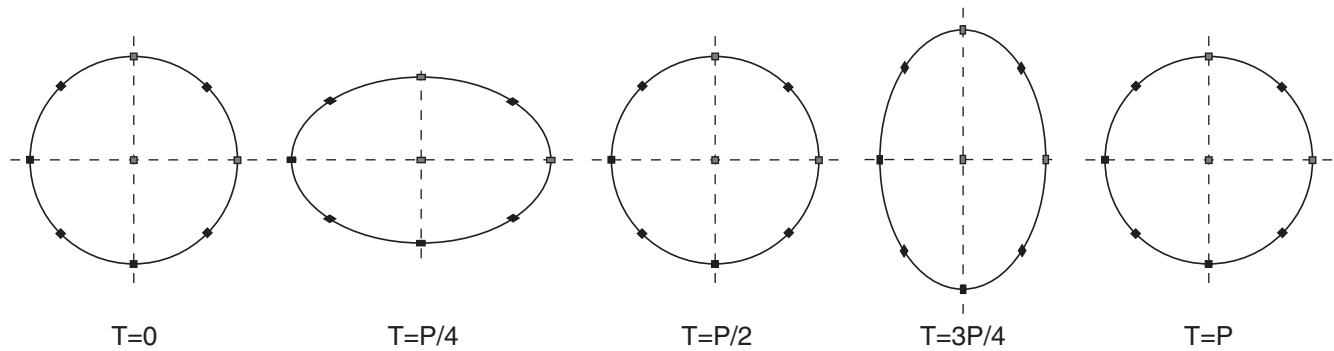
Figure 1. Deformation of a ring of particles during one period, *P*, of a passing gravitational wave. The wave would be traveling through the page causing a transverse distortion of space. For circular ring at time $T = 0$, the wave distorts it into an ellipse, first one direction and then the other. Note: this sketch shows the effect of a wave in the plus polarization.

waves (like electromagnetic waves). A passing gravitational wave causes a differential strain in space perpendicular to the propagation direction of the wave. Thus, if there were a circular ring of masses in space, a passing gravitational wave would distort the ring into an ellipse, as shown in Figure 1. As several cycles of the wave travel by, the axes of the ellipse would oscillate. The amplitude of the wave is typically characterized by the strain, *h*, or relative length change of the axes of the ellipse. The Initial LIGO detector has now achieved its design sensitivity and can detect, with good signal-to-noise ratio, a strain of $h \approx 10^{-21}$ around 100 Hz, which is equivalent to the waves produced by an inspiraling pair of neutron stars within about 49 million light years of the Earth.

The LIGO detectors use laser interferometers to measure the differential change in the distance between two pairs of mirrors 4 km apart. Figure 2 shows the basic layout of the detector; it is essentially a Michelson interferometer, but several optical components have been added to improve the signal-to-noise ratio of the detector. Laser light enters through the power recycling mirror on the left and is split into the two arms by a beam splitter. Half the light goes into each arm, where it resonates in a 4 km long Fabry–Perot cavity. An optimally oriented gravitational wave will compress one arm and stretch the other, introducing a differential phase shift on the light returning from the arms to the beam splitter. The phase shift changes the interference condition, and these changes are detected by photodiodes at the output port. The mirrors are controlled so that most of the light returning from the arms to the beam splitter goes back toward the laser, which allows the power recycling mirror to resonantly capture the light and store it in the interferometer. Simply stated, when a gravitational wave passes through the detector each test-mass mirror remains locally at rest, but the distance between them changes. If the wave is large enough, then the photodetectors at the output should be able to measure the change in the interference condition due to the distance change and distinguish that signal from background noise.

LIGO operates interferometric detectors at two facilities. One facility is located in Livingston Parish, Louisiana, about 20 miles east of Baton Rouge and operates a single 4 km baseline interferometer. The second LIGO facility is located on the Hanford Site in eastern Washington state. That facility operates both a 4 km baseline interferometer and a 2 km baseline interferometer running side by side in the same vacuum system. The Initial LIGO detectors have been running in this configuration for some time, and as of 30 September 2007 have collected one integrated year of triple-coincident data (i.e., with all three interferometers running in science mode) at the design sensitivity. We are now in the process of enhancing the performance of the two 4 km interferometers to increase the range by at least a factor of 2. Because the distribution of galaxies within 100 million light years of the Earth is not uniform (Powell, 2008), the number of Milky Way equivalent galaxies, and hence the expected number of sources within a distance *d* of the Earth, scales approximately as $d^{2.7}$ (Nutzman *et al.*, 2004), so doubling the sensitivity should improve the detection rate by about a factor of 6.5.
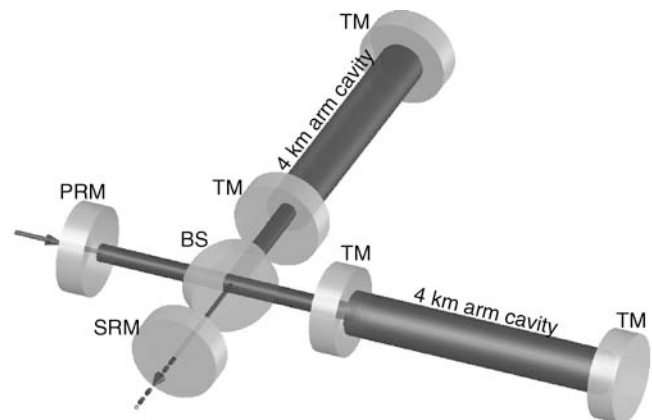
Figure 2. Schematic view of the main optics for Advanced LIGO. The laser light enters from the left, passes through the power recycling mirror (PRM), and continues to the beam splitter (BS). The beam splitter splits the light into the two 4 km Fabry–Perot arm cavities where the light resonates between the test-mass mirrors (TM). Gravitational-wave signals are detected on the light passing thought the signal recycling mirror (SRM) to the output port.

The LIGO lab has recently begun the construction of Advanced LIGO (Fritschel, 2003), a major upgrade to the Initial LIGO detectors, which will begin installation in 2011. The goal is to make the detection of gravitational waves a regular event and to make the analysis of gravitational-wave signals a powerful new tool for astronomy. To achieve this we plan to improve the signal-to-noise ratio in the existing detection band by about a factor of 10 and to move the low-frequency edge of the detection band from 40 to 10 Hz, which will allow us to start tracking the final inspiral of compact binary systems earlier in their evolution. The anticipated improvement in sensitivity along with the estimated signal strengths for several sources are shown in Figure 3. Improving the lower edge of the detection band to 10 Hz will also allow us to observe the inspirals not only of pairs of neutron stars but also of binary systems containing more massive objects such as black holes with 10 to 30 times the mass of the sun. The facilities and vacuum equipment (shown in Fig. 4) will remain essentially unchanged, but most of the detector systems such as lasers, optics, seismic isolation, and control systems will be upgraded. Additional optics will be added to the interferometer configuration, and the optical configuration will be improved.
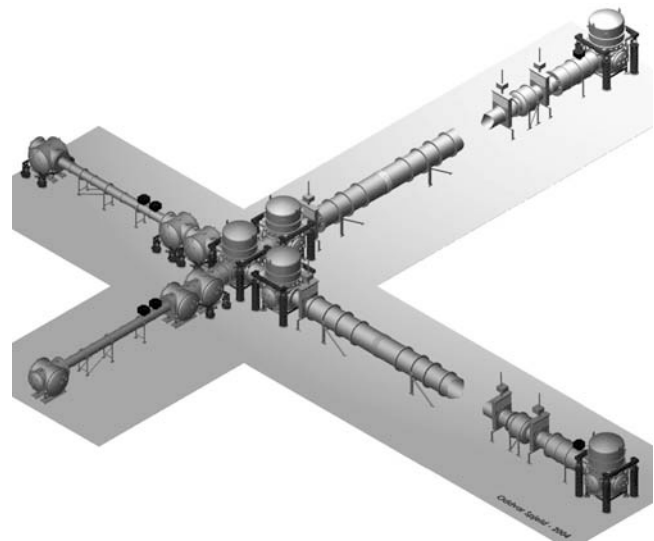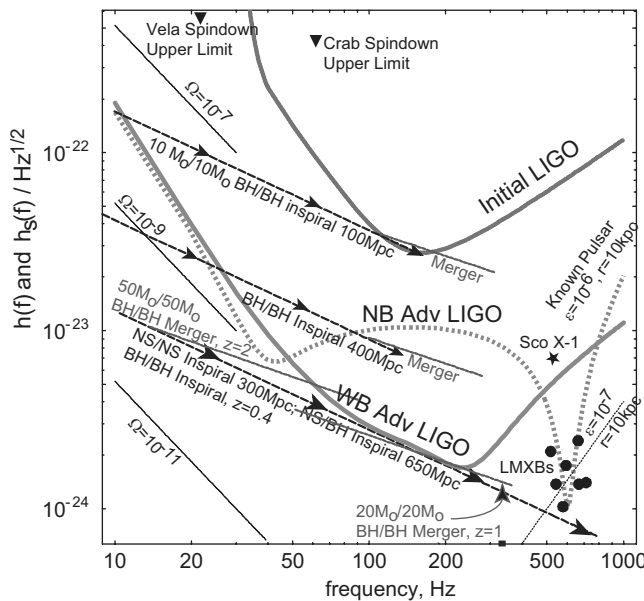

Figure 4. Layout of the LIGO vacuum equipment. The five large chambers (e.g., chambers at the top right, bottom right, and center) are the BSC and hold the beam splitter and test-mass mirrors. The six smaller chambers on the left-hand side are the HAM chambers and are used to hold other components of the interferometer. For scale, the BSC are about 5.5 m tall and the circular doors on the side of the HAM chambers are about 2.1 m in diameter.

Seismic Isolation and Alignment for Advanced LIGO

The requirements for the motion of the Advanced LIGO mirrors are very strict. The Advanced LIGO interferometer cannot distinguish between differential length changes in the

Figure 3. Predicted sensitivity of Initial LIGO, Advanced LIGO tuned for wideband (WB) performance, and Advanced LIGO tuned for narrowband (NB) performance. A variety of astrophysical sources are shown. The performance of the Advanced LIGO detector should make the detection of gravitational waves a regular event.

arms caused by the space-time distortion of a passing gravitational wave and differential length changes caused by mirror motion. Note that for an interesting discussion about interferometer configurations where this might not be true, see recent work by Kawamura, Chen, and others (Kawamura and Chen, 2004). The inability to distinguish between mirror vibrations (e.g., from seismic noise) and gravitational waves means that Advanced LIGO must use a high performance isolation and alignment system to support and isolate the test-mass mirrors (Robertson *et al.*, 2004). To meet the Advanced LIGO sensitivity goals, the system must isolate the mirrors from ground vibrations and provide quiet actuation and alignment for the mirrors so the resonance conditions for the LIGO cavities can be acquired and maintained. At 10 Hz the motion of the test-mass mirrors must be less than 1×10^{-19} m/$\sqrt{\text{Hz}}$, approximately nine orders of magnitude less than the typical ground motion at the observatories at that frequency (Fritschel *et al.*, 2001).

Planned Isolation Platforms for Advanced LIGO

Not only must the optics be kept still in the gravitational-wave detection band from 10 Hz up to several kilohertz, but it is also important to minimize their relative motion below 10 Hz. Because the interferometer comprises a set of coupled resonant optical cavities, as the interferometer moves away from the correct operating point there is nonlinear coupling of mirror motion to signal in the gravitational-wave detection readout signal. In the most extreme example, if the round trip distance between the two mirrors in one arm changes by

$\lambda/F \approx 2$ nm, where λ is the wavelength of the laser light (1.064 μm) and F is the cavity finesse (about 450), the light will not resonate in the arms and the interferometer will not function.

To hold the coupling of various noise sources to an acceptable level, the length fluctuations of the 4 km arms must be below 1×10^{-14} m rms, despite, for example, diurnal tidal distortions of the ground of approximately 200 μm. The proposed seismic isolation and suspension system for the Advanced LIGO test masses uses a set of seven layered stages: an external hydraulic stage (one layer), an in-vacuum active isolation system (two layers), and a quadruple pendulum (four layers), which supports the 40 kg test mass. Every layer provides additional isolation from both ground motion and the previous layer. LIGO has divided this system into two subsystems: Seismic Isolation, consisting of the external hydraulic external pre-isolator (HEPI) (Hardham *et al.*, 2004, 2006) and the in-vacuum active isolation stages (Abbott *et al.*, 2004), and Suspensions, consisting of the multiple pendulum stages (Robertson *et al.*, 2002).

In addition to the main optics there are a considerable number of auxiliary optics, which must also be isolated from ground motion. For example, these include the power and signal recycling mirrors, the optics that prepare the light for injection into the main portion of the interferometer, and the optical filters and photodiodes for the light containing the gravitational-wave information. Most of the auxiliary optics are placed in smaller vacuum chambers that are called horizontal access module (HAM) chambers. A simpler seismic isolation system is used for these optics. This consists of a HEPI system external to the chamber, a single layer active platform within the chamber, and various one, two, or three stage pendulums for the various optics depending on the required isolation performance. Drawings of the two isolation platform designs are shown in Figure 5.

Requirements for Translation Motion of the BSC and HAM systems

The goal of the seismic isolation subsystem is to provide a quiet, well-controlled platform to support the various optical components. The noise requirements for the platforms are shown in Figure 6. The chambers are mounted on the technical slab, which is nominally separate from the slab for the building. Because the motion of the technical slab at 1 Hz (particularly the Livingston Observatory) can be 1×10^{-8} m/$\sqrt{\text{Hz}}$, the HAM platform should provide at least a factor of 25 isolation from floor motion at 1 Hz, and the basic symmetric chambers (BSC) platform should provide a factor of 1000 (Fritschel *et al.*, 2001).

The frequency-dependent nature of the coupling between tilt and a seismometer's horizontal signal (see the Derivation of the Rotation Requirement section) means that the isolation requirements that are relevant to tilt are those below 1 Hz. At 0.1–0.2 Hz the goals for the BSC and HAM are typically a factor of 10–20 below the typical motion at the Livingston Observatory. Because the isolation at these frequencies is done actively, we need to measure the ground motion at the 2×10^{-7} m/$\sqrt{\text{Hz}}$ level and actively correct the platform to compensate for this motion. Below about 0.4 Hz the motion goals for the platforms should be read as applying to the differential motion between adjacent systems, whereas at 0.4 Hz and above they should be read as applying to the inertial motion of each individual platform. This distinction is drawn because we are trying to minimize the differential motion between the various optics at low frequency, so moving all the optical platforms together is acceptable. However, at frequencies above about 0.4 Hz, the various suspensions for the optical systems each have their own dynamics, so the common-mode motion of the plat-
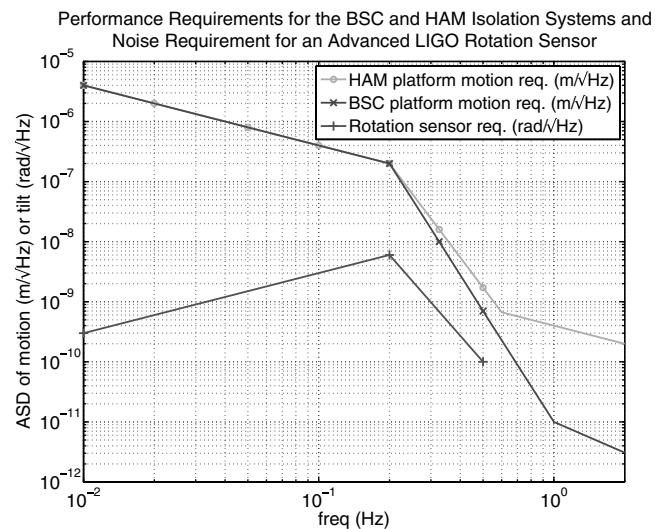

Figure 5. Computer-aided design renderings of the isolation platforms for the BSC (left-hand side) and HAM chamber (right-hand side). The top of the BSC has been rendered transparent to show the isolation platform. The doors and external supports of the BSC are not shown. The HAM platform is shown in a sectioned HAM chamber.

Figure 6. Performance goals for the BSC and HAM isolation systems below 2 Hz. These motion goals are used to set a requirement for a rotation sensor for Advanced LIGO, which is also shown.

forms at these frequencies and above can generate differential motion of the optics.

Our control systems work as single-input single-output controllers for each degree of freedom (DOF). We generate the sensor signal by using two types of sensors. We use relative displacement sensors at low frequency to measure the motion of the isolation platform with respect to its support structure (the HEPI support structure is attached to the building slab). We use inertial sensors (seismometers) to measure the motion of the ground and to measure the inertial motion of the isolated tables. We use ground seismometers as feedforward sensors, and we use seismometers on the isolated platform as feedback sensors for the active isolation loops. Because the performance of active systems is limited by the performance of the sensors, we have a long-standing interest in high performance inertial instruments.

The first demonstration of active seismic isolation at 0.1–0.3 Hz (around the microseismic peak) in all three translation directions was done in our lab at Stanford (Hua, Adhikari, *et al.*, 2004). The noise floor of the Streckeisen STS-2 used to measure our slab motion is perfectly adequate to achieve the Advanced LIGO performance requirements. The difficulty arises when one attempts to achieve good performance at the microseism and not suffer from large motions of the platform at somewhat lower frequencies, which result from the sensitivity of the STS-2 to slab rotations.

Derivation of the Rotation Requirement

The major impediment to achieving good isolation below 100 mHz is the sensitivity of the horizontal accelerometers to rotation. If we were able to independently measure the rotation, we could calculate the true translation motion. The rotation measurement requirement is set by simply calculating how much erroneous rotation signal can be present in the translation measurements and still meet the isolation goals for Advanced LIGO.

Review of Tilt-Horizontal Coupling

It is well known that horizontal seismometers are sensitive to tilt. This can be demonstrated with a simple example system: a horizontal mass-spring system on a tilting floor. This system has a mass, m, on a spring, k, with damping, b. The mass is free to slide on the floor. The mass location is x_m, and the attachment point to the floor is x_f. The floor is allowed to tilt with respect to local gravity g by an angle θ. Because the motions are all small, we ignore centrifugal forces. The basic equation describing this system is

$$m\ddot{x}_m = -k(x_m - x_f) - b(\dot{x}_m - \dot{x}_f) + mg\sin(\theta) + F_{\text{ext}}. \tag{1}$$

We define the x_d as the differential motion $x_m - x_f$ between the mass and the floor. F_{ext} represents the effect of an exter-

nal force applied directly to the mass and is used for analysis in the next section. A measurement of x_d or $\dot{x}_d$ could be used as a direct measure of floor motion (or velocity). Alternatively, x_d could be controlled with a servo and the control signals used to derive the force (or tilt) applied by floor motion. We let θ be small, and we take the Fourier transform so that $\dot{x}_m$ becomes iwx_m, et cetera. We can then rewrite equation (1) as

$$x_d = \frac{-\omega^2}{\omega^2 - i\omega b/m - k/m}\left(x_f - \frac{g}{\omega^2}\theta + \frac{F_{\text{ext}}}{m\omega^2}\right). \tag{2}$$

The differential motion is sensitive to both floor motion and floor tilt. The dynamics of the particular device are contained in the first term, and the relative sensitivity to translation and tilt are contained in the second term. This is a specific example of the general result that, for a horizontal seismometer, the ratio of the sensitivity to rotation (seismometer signal per radian of angle) to the sensitivity to horizontal motion (seismometer signal per meter of translation) at a particular frequency ω (in rad/sec) is

$$\frac{\text{rotation response}}{\text{translation response}} = -\frac{g}{\omega^2}. \tag{3}$$

Thus, we expect that in our laboratory environment below some frequency the signal from our horizontal seismometers will be dominated by rotation. For pure translation motion, the noise floor of the commercially available instruments is sufficient to meet the Advanced LIGO noise specifications. The tilt motion of the slab confuses the sensors and can cause the system to execute spurious translations in response to low-frequency tilts.

Rotation Sensing Requirement

Therefore, we would like to have sensors that can measure the ground rotations about the horizontal axes so that we can remove this signal in real time from the horizontal seismometers and use only the true ground translation to control the isolation system. For example, if the rotation sensor output is calibrated in radians and the translation sensor output is calibrated in meters, the signal from the rotation sensor would be band-pass filtered, integrated twice, scaled by local gravity, and subtracted from the translation sensor in real time. It should be noted that not all sensors generate signals in radians or meters, so the correct number of integrations may not be two. It could be true that reducing the number of integrations has benefits for the overall performance. Figure 6 shows the horizontal motion goals for the isolation platforms in the two chambers. The goal for the platform in the BSC chamber is more strict, so we follow that goal curve.

For the unresolved ground tilt to never exceed the translation motion goal of the seismic isolation system, the required noise floor of the rotation sensor is

rotation sensing req. (rad/$\sqrt{\text{Hz}}$)

$$= \frac{1}{5} \times \frac{\omega^2}{g} \times \text{platform motion goal (m/} \sqrt{\text{Hz}}). \quad (4)$$

We use a safety factor of 5 so that the coupling of rotation noise to translation is well below the translation motion goal, and so that in the 40–100 mHz band the amplification of 4 caused by the filter applied to the horizontal ground-motion sensor (described in the next section) will be below the motion goal. We also round down the calculated numbers to simplify the communication of the requirement (e.g., we set the 10 mHz level to be 3×10^{-10} rad/$\sqrt{\text{Hz}}$ rather than 3.22×10^{-10} rad/$\sqrt{\text{Hz}}$. The amplitude spectral density (ASD) of the allowed noise for the three points on the requirement curve is shown in Table 1.

We do not set a requirement below 10 mHz because at those frequencies the control loops for the isolation systems are controlled by the displacement sensors, and the location commands are provided by the global interferometer control system. We also do not set a requirement above 0.5 Hz because at these frequencies we can already control the tilt performance with the feedback seismometers located in the vacuum system. These sensors include differential vertical seismometers (Streckeisen STS-2s and Geotech GS-13s with custom readouts), which are capable of measuring and directly controlling tilt to the required level.

Equation (4) assumes that the local gravity field, g, is constant. It is interesting to consider the impact that variations in the local gravity field would have on the performance of the scheme to compute the true local ground translations. There are two potentially important ways in which the local gravity vector may change. The first is that the magnitude of the vertical component may vary. This may result from various environmental effects such as atmospheric loading. These effects have been measured to change the local gravity by 3–6 micro gal (van Dam and Wahr, 1987) (3–6×10^{-8} m/sec^2). This changes the scale factor for the correction term, but we will see subsequently that we only need to have the scale factor for g correct to about 1% in order to meet the Advanced LIGO requirements, so these small changes will not pose a problem. The other issue is time-varying horizontal components of local gravity, which affect the horizontal seismometer but not the rotation sensor. Hughes and Thorne have made estimates for these local gravity components, as they will directly affect the main LIGO optics (Hughes and Thorne, 1998). They show that for passing seismic waves, which generate a horizontal surface displacement with ASD $W(f)$ m/$\sqrt{\text{Hz}}$, the horizontal grav-

itational force on a mass, m, from the time-varying density distributions of the ground is approximately

$$F_{\text{ext}} \approx 4\pi m G \rho \beta(f) W(f), \quad (5)$$

where G is Newton's constant, ρ is the average ground density (about 1800 kg/m^3), f is the frequency, and $\beta(f)$ is a dimensionless scaling parameter, which is a function of the ground composition and the type of surface waves currently present in the environment (because Rayleigh modes and Love modes have very different gravitational effects). They estimate β to be between 0.15 and 1.4 at noisy times.

From equation (2), we see that the relative sensitivity of a horizontal seismometer to floor displacements and to external forces on the sensor mass is $1/m\omega^2$. Therefore, we can estimate that the fraction of sensed motion, which comes from the gravity field disturbances, is

fractional error from horizontal gravity

$$\approx \frac{F_{\text{ext}}}{m\omega^2 x_f} \approx \frac{4\pi G \rho \beta(f)}{\omega^2} \approx 5 \times 10^{-4} \quad \text{at} \quad 0.01 \text{ Hz,} \quad (6)$$

which is small enough to be ignored. Hence, choosing a fixed value for g should be sufficient for our frequency band of interest.

There are several techniques that can be used in concert to maintain low relative motion between the optics in the presence of differential ground tilts. The first is to filter the signals from the horizontal seismometers as a function of frequency and to use the signal in the band where one believes the signal is dominated by true translation but reject the signal at frequencies where one believes that the tilt signals dominate. This type of filtering is used now to good effect and is described in the following section. A second technique is to measure the angular acceleration directly. We do this now with differential vertical seismometers but only at frequencies above about 0.3 Hz. We are anxious to see the improvement of sensors to expand this capability. A third approach is to measure and directly control the distances between the support points of the optics, a technique often called suspension point interferometry (Robertson *et al.*, 1983; Aso *et al.*, 2006). This technique holds great promise but currently remains in the demonstration phase. Finally, we use the interferometer controls to sense and control the distance between the optics. This is very effective but reduction of the input noise will simplify the interferometer control, make the interferometer more robust against large external disturbances, and improve our ability to get the interferometer into the operational regime to detect gravitational waves.

Discrimination with Frequency. We have developed very high performance filters to distinguish the signals at 0.1 Hz and above, which are dominated by translation, from the signals below 30 mHz, which are typically dominated by ground tilts (Hua, DeBra, *et al.*, 2004). It is unlikely that

Table 1

Frequencies and Amplitudes of the Rotation Sensing Noise Requirement

| Frequency (Hz)	0.01	0.2	0.5
Noise ASD (rad/$\sqrt{\text{Hz}}$)	3e−10	6e−9	1e−10
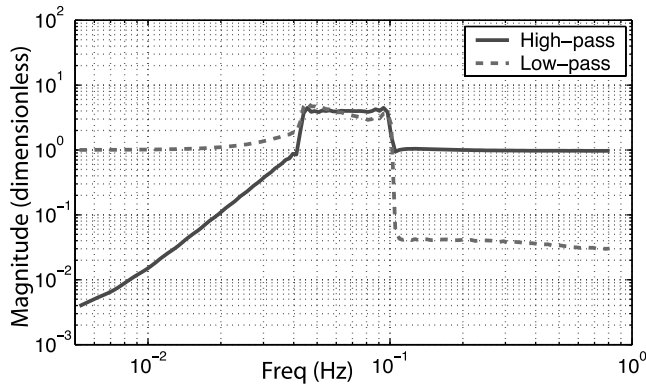
Figure 7. Polyphase FIR filter used to separate rotation and translation frequencies.

much further optimization of these filters can be done. Because the control system runs in real time, the filters used can only change gain at a finite rate as a function of frequency; therefore, if those filters have a passband close to unity at 0.1 Hz, signals at slightly lower frequencies must have a non-zero impact on the control system. We have developed a high performance filter to do this frequency discrimination, which is shown in Figure 7. Its performance below 1.9 Hz is equivalent to a finite impulse response (FIR) filter with 16,384 taps running at 64 samples/sec. Because the desired filter response above 1 Hz is a flat passband response of one, certain simplifications can be made in the implementation. We use a special computational method called a polyphase FIR filter to implement this filter (Crochiere and Rabiner, 1983; Hua, De-Bra, *et al.*, 2004).

This filter allows isolation at 0.1 Hz and above while rejecting ground rotations below about 30 mHz. This filter amplifies ground motion in the 40–100 mHz band. Because ground motion in the 40–100 mHz band is typically very small and ground motion at the microseismic peak around

0.15 Hz is large, this filter typically works very well, and systems now using this filter have dramatically improved the duty factor of the LIGO Observatory in Livingston, Louisiana (Hardham *et al.*, 2006). The shape of the filter is a compromise between isolation above 0.1 Hz, amplification of the 40–100 mHz band, and rejection of signal below 40 mHz. Further improvements to filter performance in one of these three areas results in degradation in performance in the other areas. Thus, while some tuning may help the interferometer, it is unlikely that the system performance of the interferometer can be improved very much further by simple adjustments to the filter design.

Direct Measurement of Ground Rotations. The ability to directly measure the ground rotation and use that information to correct the translation measurements would improve the performance of the isolation system. During windy times, which are common at both the Livingston, Louisiana, site and the Hanford, Washington, site, the ground tilts below 100 mHz can be quite dramatic. Figure 8 shows a horizontal measurement of each observatory slab taken during windy times by an STS-2 located near the beam splitter chamber. The wind speed for the Hanford measurement was 7.5 miles/hr. The wind at the Hanford observatory meets or exceeds this speed 35% of the time. The measurements are interpreted in two ways. First we calibrate the motion assuming the signal is truly horizontal motion. It is unlikely that it is truly translation, however, because this would imply translations of more than 100 microns RMS at 50 sec periods. Also, the Hanford interferometer was running at the time and the relative distance changes to the optics 4 km away was substantially smaller than 100 microns. Thus, it is reasonable to assume that the signal below 100 mHz contains substantial ground tilt, and so we plot the signal calibrated as ground tilt on the same figure. We do the same for a windy time at the Livingston Observatory, but we do not
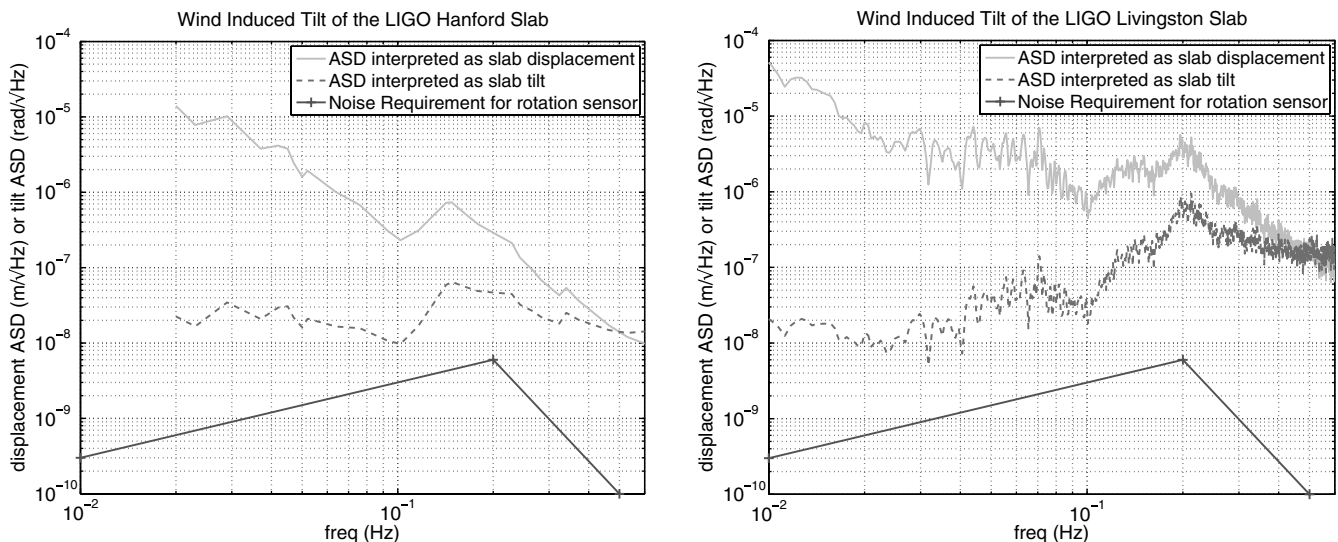
Figure 8. Wind-generated tilt of the LIGO technical slab at the two observatories.

have as complete an argument to convince us that the signal there is truly tilt because the wind prevented interferometer operation at the time. We see that in both cases the implied tilt below 100 mHz is an order of magnitude larger than the rotation sensing requirement.

Tilt in the 40–100 mHz band will be amplified by the current system. Effective rotation sensing would clearly improve the performance of the seismic isolation system during windy times.

Earthquakes are another source of energy in the 40–100 mHz band. Typically, an earthquake of about magnitude 6.5 or greater anywhere in the world will make the interferometers unusable for several hours. The loss in duty factor from wind and earthquakes during the most recent science run was about 5% (Hoak and Bland, 2008). Better rotation sensing below 100 mHz would help the interferometer in two ways. First, we can better distinguish what part of the signal in the 40–100 mHz band is from translation and what is from tilt, so we can apply the correct controls. Second, if we were able to accurately resolve tilt at 10 mHz, we could change the FIR filter so that we had less rejection of the 10–40 mHz signal and less amplification of the signals in the 40–100 mHz band.

Comparison with Existing Sensors

We do not know of any sensors that can meet these rotation sensing requirements in a configuration that is usable at the LIGO Observatories, but it is interesting to compare our requirements with a few well-known rotation sensors. One technique is to use a rotational analog of a conventional seismometer, where a proof mass is suspended on an angular pivot with a low natural frequency and the rotation of the mass is measured relative to the case (DeSalvo, 2009). An early example of the dumbbell sensor technology for use in seismic isolation systems for gravitational-wave detectors was done by Speake and Newell (Speake and Newell, 1990). The noise floor of that device was about 1×10^{-8} rad/$\sqrt{\text{Hz}}$ at 0.5 Hz and then flat at about 1×10^{-9} rad/$\sqrt{\text{Hz}}$ above 3 Hz. More recently, a group at University of Western Australia has been developing a 2-DOF version with a novel optical readout scheme for use with their low-frequency seismic isolation system (Winterflood et al., 2000; Zhou et al., 2001; Cheng et al., 2002), but that system has not yet reported performance sufficient to meet these requirements below 1 Hz.

There are also several ways to arrange conventional seismometers to measure rotations. One method is to use the differential signal from two horizontally separated vertical sensors. The LIGO technical slab is designed to be stiff; it is approximately 30 inch thick and reinforced with two layers of rebar. One could imagine that placing a vertical seismometer (e.g., an STS-2 or Trillium 240) on either side of the LIGO chamber with a 5 m separation between the sensors would be a good way to measure the slab tilt at the chamber. One can use the manufacturer's noise curves (Nanometrics, 2008) for the instrument performance to make an optimistic

model of the rotation noise for two independent sensors placed 5 m apart, so that the ASD of the rotation sensing noise floor, $\tilde{r}$ in rad/$\sqrt{\text{Hz}}$, is $\tilde{r} = (\sqrt{2}/5\text{ m}) \times \tilde{z}$, where $\tilde{z}$ is the ASD of the vertical sensor noise in m/$\sqrt{\text{Hz}}$. The resulting noise curve is shown in Figure 9. It crosses the required noise performance at about 43 mHz.

There are a variety of noise sources that make this type of measurement difficult. Perhaps the most serious is that the common-mode signal in the two sensors from vertical ground motion is substantially larger than the differential signal, which contains the tilt information. Thus, the scale factors of the two seismometers must be well matched to avoid cross coupling the vertical motion into the tilt measurement. A measurement of the vertical ground motion at the Livingston Observatory was made at two different times on the same day, once at a windy time and several hours later when the wind speed was low. In Figure 9, we plot the cross coupling from the vertical motion to the rotation measurement with a 5 m baseline between the sensors and a 0.2% difference in the scale factors. With that level of matching, the cross coupling of the vertical noise at a windy time does not violate the rotation sensing noise requirement above 43 mHz. Whether one can achieve stable matching of scale factors to this level over year-length time scales is not known.

Perhaps the most promising method of achieving the desired noise performance is with interferometric ring gyros. Work by Schreiber and others on ring laser gyros has resulted in devices capable of measuring rotation rates as small as 1×10^{-10} (rad/sec)/$\sqrt{\text{Hz}}$ (Igel et al., 2007; Stedman et al., 2007). This is comparable to the noise performance we seek. These devices are optimized for excellent stability on very long time scales but are large, sensitive about a vertical axis, and not adapted for our laboratory environment. However, work on the GEOsensor project (Schreiber et al., 2005) to
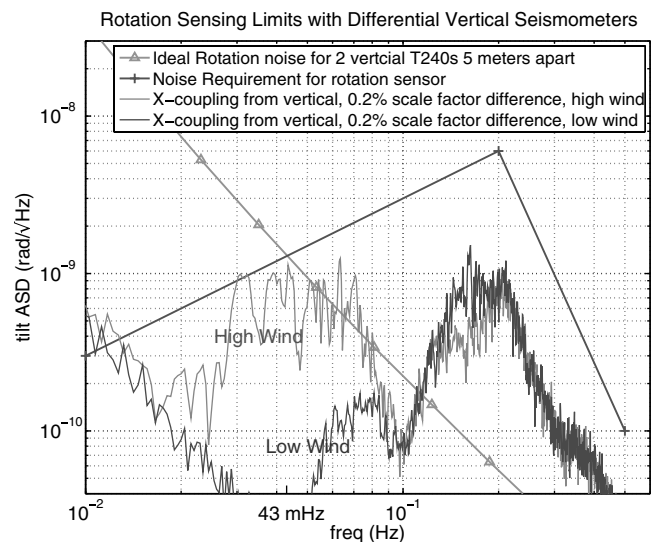
Figure 9. Using a pair of Trillium 240s as an Advanced LIGO rotation sensor.

adapt this technology to a device designed for codeployment with a low-frequency seismometer is very exciting.

Conclusions

The construction of the Advanced LIGO interferometers will make the detection of gravitational waves from astrophysical sources a regular occurrence. The seismic isolation system used to help isolate optics will be improved if a high performance rotation sensor for the ground can be developed to sense the ground tilts between 10 and 500 mHz. We derive the requirements for a sensor, which will guarantee that unresolved ground tilt will never compromise the performance of the isolation system. Such sensors would improve the interferometer reliability and ease of use, especially during windy times or after medium to large earthquakes anywhere in the world. However, we see that these requirements are difficult to achieve and note in closing that even modest improvements in our ability to measure rotations below 500 mHz would be useful, both to improve system performance and to improve our understanding of the environmental disturbances.

Data and Resources

The wind induced ground tilt measurements at the LIGO Hanford Observatory are available at the Observatory's online logbook. The logbook can be found at http://ilog.ligo-wa.caltech.edu/ilog/ and can be read by the public. The log entries are in the Detector logbook on 14 April 2001, with additional information in entries on 14 April 2008. Other data used in this article are available from the first author.

Acknowledgments

References

Abbott, R., *et al.* (2004). Seismic isolation enhancements for Initial and Advanced LIGO, *J. Quant. Gravity* **21,** S915–S921.

Acernese, F., *et al.* (2008). Status of Virgo, *Class. Quant. Gravity* **25,** no. 11, 114,045.

Aso, Y., M. Ando, S. Otsuka, and K. Tsubono (2006). Active vibration isolation using a suspension point interferometer, *J. Phys.* Conference Series, **32,** 451–456.

Barish, B., and R. Weiss (1999). LIGO and the detection of gravitational waves, *Phys. Today* **52,** 44–50.

Barriga, P., *et al.* (2005). Technology developments for ACIGA high power test facility for advanced interferometry, *Class. Quant. Gravity* **22,** no. 10, S199–S208.

Cheng, Y., J. Winterflood, L. Ju, and D. G. Blair (2002). Tilt sensor and servo control system for gravitational wave detection, *Class. Quant. Gravity* **19,** no. 7, 1723–1729.

Crochiere, R. E., and L. R. Rabiner (1983). *Mulitrate Digital Signal Processing*, Prentice-Hall, Englewood Cliffs, New Jersey, 79–88.

DeSalvo, R. (2009). Review: accelerometer development for use in gravitational wave-detection interferometers, *Bull. Seismol. Soc. Am.* **99,** no. 2B, 990–997.

Fritschel, P., D. Coyne, J. Giaime, B. Lantz, and D. Shoemaker (2001). Seismic isolation subsystem design requirements document, *LIGO Internal Document E990303-03-D*, available at http://admdbsrv.ligo.caltech.edu/dcc/.

Fritschel, P. (2003). Second generation instruments for the Laser Interferometer Gravitational-wave Observatory (LIGO), in Gravitational-Wave Detection, *Proc. SPIE* **4856,** 282–291.

Grote, H., and LIGO Scientific Collaboration (2008). The status of GEO 600, *Class. Quant. Gravity* **25,** no. 11, 114,043.

Hardham, C., *et al.* (2004). Multi-DOF isolation and alignment with quiet hydraulic actuators, in Spring Topical Meeting on Control of Precision Systems, *Proc. ASPE*, **32,** 127.

Hardham, C., *et al.* (2006). Quiet hydraulic actuators for LIGO, in Mechatronics 2006, *4th IFAC-Symposium on Mechatronic Systems*.

Hoak, D., and B. Bland (2008). Downtime accounting in S5, *LIGO Internal Document T080160-00-D*: available at http://admdbsrv.ligo.caltech.edu/dcc/.

Hua, W., R. Adhikari, D. DeBra, J. Giaime, G. Hammond, C. Hardham, M. Hennessy, J. How, B. Lantz, M. Macinnis, R. Mittleman, S. Richman, N. A. Robertson, J. Rollins, D. H. Shoemaker, and R. Stebbins (2004). Low frequency active vibration isolation for Advanced LIGO, in Gravitational-Wave and Particle Astrophysics Detectors, *Proc. SPIE* **5500,** 194.

Hua, W., D. DeBra, C. T. Hardham, B. Lantz, and J. Giaime (2004). Polyphase FIR complementary filters for control systems, in Spring Topical Meeting on Control of Precision Systems, *Proc. ASPE* 32, 109–114.

Hughes, S. A., and K. S. Thorne (1998). Seismic gravity-gradient noise in interferometric gravitational-wave detectors, *Phys. Rev. D* **58,** no. 12, 122,002.

Igel, H., A. Cochard, J. Wassermann, A. Flaws, U. Schreiber, A. Velikoseltsev, and N. Pham Dinh (2007). Broadband observations of earthquake-induced rotational ground motions, *Geophys. J.* **168,** 182–196.

Kawamura, S., and Y. Chen (2004). Displacement-noise-free gravitational-wave detection, *Phys. Rev. Lett.* **93,** no. 21, 211,103.

Kuroda, K., and The LCGT Collaboration (2006). The status of LCGT, *Class. Quant. Gravity* **23,** no. 8, S215–S221.

Nanometrics (2008). Nmx-trillium-6-pager.pdf, *Manufacturers Specification*, available at http://www.nanometrics.ca.

Nutzman, P., V. Kalogera, L. S. Finn, C. Hendrickson, and K. Belczynski (2004). Gravitational waves from extragalactic inspiraling binaries: Selection effects and expected detection rates, *Astrophys. J.* **612,** 364–374.

Powell, R. (2008). *Atlas of the Universe*, http://www.atlasoftheuniverse.com/, R. Powell has assembled a beautiful collection of maps of the universe.

Robertson, N. A., *et al.* (2002). Quadruple suspension design for Advanced LIGO, *Class. Quant. Gravity* **19,** no. 15, 4043–4058.

Robertson, N. A., *et al.* (2004). Seismic isolation and suspension systems for Advanced LIGO, in Gravitational-Wave and Particle Astrophysics Detectors, J. Hough and G. Sanders (Editors), *Proc. SPIE* **5500,** 81.

Robertson, N. A., R. W. P. Drever, I. Kerr, and J. Hough (1983). Passive and active seismic isolation for gravitational-radiation detectors and other instruments, *J. Phys. E: Sci. Instrum.* **15,** 1101–1105.

Schreiber, U., H. Igel, A. Cochardand, A. Velikoseltsev, A. Flaws, B. Schuberth, W. Drewitz, and F. Muller (2005). The GEOsensor project: A new observable for seismology, in *Observation of the System Earth from Space*, Springer, New York.

Shaddock, D. A. (2008). Space-based gravitational-wave detection with LISA, *Class. Quant. Gravity* **25,** no. 11, 114,012.

Sigg, D., and LIGO Scientific Collaboration (2008). Status of the LIGO detectors, *Class. Quant. Gravity* **25,** no. 11, 114,041.

Speake, C. C., and D. B. Newell (1990). The design and application of a novel high-frequency tiltmeter, *Rev. Sci. Instrum.* **61,** 5, 1500–1503.

Stedman, G. E., R. B. Hurst, and K. U. Schreiber (2007). On the potential of large ring lasers, *Opt. Commun.* **279,** 124–129.

Tatsumi, D., *et al.* (2007). Current status of Japanese detectors, *Class. Quant. Gravity* **24,** no. 19, S399–S403.

Taylor, J. H., and J. M. Weisberg (1989). Further experimental tests of relativistic gravity using the binary pulsar PSR 1913 + 16. *Astrophys. J.* **345,** 434–450.

van Dam, T. M., and J. M. Wahr (1987). Displacements of the Earth's surface due to atmospheric loading-effects of gravity and baseline measurements, *J. Geophys. Res.* **92,** 1281–1286.

Winterflood, J., Z. B. Zhou, L. Ju, and D. G. Blair (2000). Tilt suppression for ultra-low residual motion vibration isolation in gravitational-wave detection, *Phys. Lett. A* **277,** 143–155.

Zhou, Z. B., J. Winterflood, L. Ju, and D. G. Blair (2001). Investigation of a laser walk-off angle sensor and its application to tilt measurement in gravitational-wave detectors, *Phys. Lett. A* **280,** 197–203.

Stanford University
Ginzton Lab
Stanford, California 94305
BLantz@Stanford.edu
    (B.L., D.E.C., D.D.)

University of Oregon
Eugene, Oregon 97403
    (R.S.)

LIGO—Livingston Observatory
Livingston, Louisiana 70754
    (B.O.)